Journal of Applied Mechanics and Technical Physics, Vol. 50, No. 4, pp. 617–627, 2009

DETERMINING THE LIMITING SOLUTIONS OF NONSTATIONARY AXISYMMETRIC HELE-SHAW PROBLEMS

V. P. Zhitnikov, O. R. Zinnatullilna, S. S. Porechnyi, and N. M. Sherykhalina

UDC 532.5

Numerical solution of the Hele-Shaw problem reduces to solution of three boundary-value problems of determining analytic functions of a complex variable in each time step: conformal mapping of the range of the parametric variable to the physical plane, the Dirichlet problems for determining the electric-field strength, and the Riemann–Hilbert problem for calculating partial time derivatives of the coordinates of points of the interelectrode space (the images of the points on the boundary of the parametric plane are fixed). Unlike in the two-dimensional problem, the electric-field strength is determined using integral transformations of an analytic function. Approximation by spline function is performed, and more accurate and steady (than the well-known ones) general solution algorithms for the nonstationary axisymmetric problems are described. Results of a numerical study of the formation of stationary and self-similar configurations are presented.

Key words: *axisymmetric Hele-Shaw problem, nonstationarity, numerical investigation.*

Introduction. Problems for the Laplace equation with moving boundaries in which the velocity of motion of the boundary is proportional to the potential gradient Φ are called the Hele-Shaw free-boundary problems. Solutions of these problems can be treated as viscous fluid flows [1–3], metal dissolution processes in electrochemical machining [4, 5] and other processes [6–8]. In the present paper, the problem is formulated with reference to electrochemical machining.

Investigation of the shaping of the free surface is significantly complicated by the need to perform complex calculations of the formation of the final configurations. For example, in a calculation of the coordinates of the surface with accuracy to 12–14 decimal places, the parameter λ of the exponential time dependence of the surface curvature at a point $e^{-\lambda t}$ can have only 1–2 exact decimal places.

Solutions of Hele-Shaw problems have previously been obtained using the finite-difference and finite-element methods [9, 10] and the boundary-element method [11–14]. Nevertheless, the methods developed earlier do not have sufficient stability against error accumulation in calculations of long transition processes.

The purpose of the present work is to develop numerical analytical methods and to study the time characteristics of the processes of formation of stationary, self-similar, and final configurations.

1. General Formulation of the Problem. During electrochemical machining, the machined surface is the anode, and the tool electrode is the cathode. After the interelectrode space is filled with an electrolyte and the electrodes are connected to a current source, there is dissolution of the anode material. The dissolution rate V — the velocity of motion of each point of the boundary (along the normal) — is defined by the Faraday law (written with the Ohm law taken into account):

$$V = kE_n. \tag{1}$$

Here k is the electrochemical constant and E_n is the electric-field strength component normal to the boundary.

Ufa State Aviation Technical University, Ufa 450000; zhitnik@mail.ru. Translated from Prikladnaya Mekhanika i Tekhnicheskaya Fizika, Vol. 50, No. 4, pp. 87–99, July–August, 2009. Original article submitted December 17, 2007; revision submitted May 14, 2008.

0021-8944/09/5004-0617

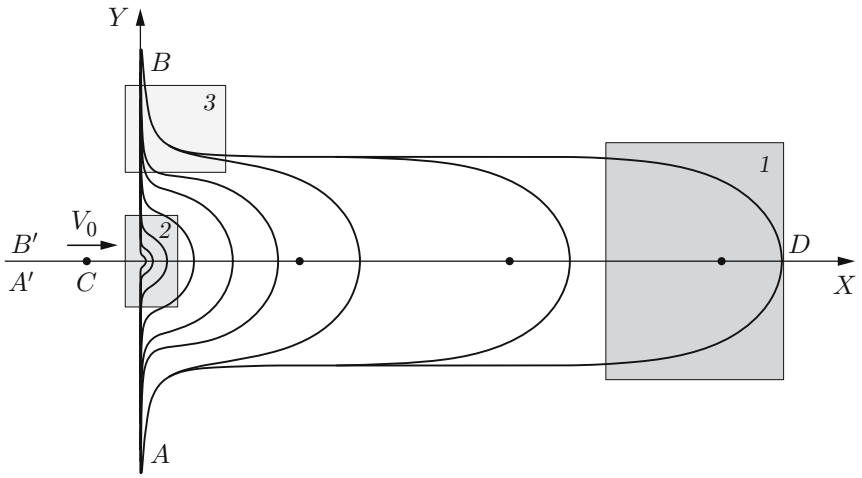

Fig. 1. Meridional section of the interelectrode space: 1) zone of stationary process; 2) zone of self-similarity (singularity); 3) final zone; ADB is the free boundary; the point C is a point source which moves at a velocity V_0 to the free surface.

The required shape of the machined surface can be obtained by choosing the shape of the tool electrode and the trajectory of its motion.

We consider the problem of shaping of a free (machined) surface by a moving point source — a needle electrode (NE). The meridional section of the interelectrode space (IES) is shown in Fig. 1.

The ideal model of the process assumes constant electrical conductivity of the electrolyte in time and space. Since the dissolution rate is low (usually a few millimeters per minute), the electric field is considered quasistatic. In this case, the electric strength vector field is potential and solenoidal. The potential Φ and the stream function Ψ of the axisymmetric field satisfy the equations

$$\frac{\partial\Phi}{\partial X}=\frac{1}{Y}\frac{\partial\Psi}{\partial Y},\qquad \frac{\partial\Phi}{\partial Y}=-\frac{1}{Y}\frac{\partial\Psi}{\partial X}. \tag{2}$$

The solution of the nonstationary problem reduces to a search for the functions $\Phi(X,Y,t)$ and $\Psi(X,Y,t)$ which satisfy Eqs. (2) in the IES (whose shape depends on time t) under definite boundary conditions. In the case of an ideal process, the boundary conditions are given as the conditions of constant values for the function $\Phi(X,Y,t)$ on the boundaries corresponding to the electrode surfaces and the function $\Psi(X,Y,t)$ on the isolated (impenetrable) boundaries. The change in the boundary shape is defined by the Faraday law (1), where $E_n=\partial\Phi/\partial n$. The initial shape of the machined surface, and the shape and velocity (trajectory) of motion of the tool electrode are specified.

The potential difference between the anode and the cathode is equal to the voltage applied to them U. If the size of the cathode is smaller than the characteristic distance to the anode, the tool electrode can be considered a point one. Then, the potential of the tool electrode is equal to $-\infty$ and the difference between the values of the stream function on the axis at the left and at the right of the source is equal to the ratio of the current strength I to the electrical conductivity of the electrolyte $\varkappa$.

It is of interest to study the variation in the shape of the boundary in time. Figure 1 shows three zones formed by different methods: 1) zone of the stationary process, in which the surface shape near the PE ceases to vary in spite of dissolution and is only shifted together with the NE; 2) zone of formation of the final shape, which do not vary after the end of dissolution; 3) zone of singularity, which is formed only if, at the initial time, the PE touches the machined surface. In this case, in the vicinity of the surface, a self-similar process occurs instantaneously, in which the geometrical similarity of the IES is preserved.

2. Polozhii Transformations. The potential and stream function of an axisymmetric field can be expressed in terms of the analytic function $f(Z)$ of the complex variable $Z=X+iY$ in a region whose boundaries coincide in shape with the boundaries of the interelectrode space in the meridional section by using the following formulas (Polozhii integral transformations [15]):

$$\Phi(X_0, Y_0) = -\frac{1}{\pi} \operatorname{Im} \int\limits_{\infty}^{Z_0} f(Z) \frac{dZ}{\sqrt{(Z - Z_0)(Z - \overline{Z}_0)}}; \tag{3}$$

$$\Psi(X_0, Y_0) = \frac{1}{\pi} \operatorname{Im} \int\limits_{\infty}^{Z_0} f(Z) \frac{(Z - X_0)\, dZ}{\sqrt{(Z - Z_0)(Z - \overline{Z}_0)}}. \tag{4}$$

Here $Z_0 = X_0 + iY_0$ and $\overline{Z}_0 = X_0 - iY_0$.

Thus, solution of the axisymmetric problems reduces to solution of a certain plane problem of determining the analytic function $W(Z)$ which is a complex potential of a certain auxiliary plane field. The potential and stream function of axisymmetric flow are obtained by the integral transformations (3) and (4) of the function $f(Z) = dW/dZ$ [16]. In particular, for a point source located at the point $X_C + i0$, we have

$$\Phi(X_0, Y_0) = -\frac{1}{4\pi\sqrt{(X_0 - X_C)^2 + Y_0^2}}, \qquad \Psi(X_0, Y_0) = \frac{1}{4\pi} - \frac{X_0 - X_C}{4\pi\sqrt{(X_0 - X_C)^2 + Y_0^2}},$$

$$W(Z) = \frac{1}{2\pi} \ln (Z - X_C), \qquad f(Z) = \frac{1}{2\pi(Z - X_C)}.$$

According to [16], on the segment $(CD]$ of the real axis,

$$\Phi(X_0, 0) = -f(X_0 + i0)/2, \qquad \Psi(X_0, 0) = 0.$$

The boundary conditions of the auxiliary plane problem are written as the integral equations obtained by setting the right sides of (3) for equipotential boundaries or the right sides of (4) for impenetrable boundaries equal to a constant. Equality to zero of the imaginary or real part of $f(Z)$ generally does not imply that the corresponding integrals are equal to zero or a constant.

The longitudinal and radial strength components [16] are determined from formulas (3) and (4):

$$E_x = \frac{\partial \Phi}{\partial X_0} = -\frac{1}{\pi} \operatorname{Im} \int\limits_{X_1 + i0}^{X_0 + iY_0} \frac{df}{dZ} \frac{dZ}{\sqrt{(Z - Z_0)(Z - \overline{Z}_0)}}; \tag{5}$$

$$E_y = \frac{\partial \Phi}{\partial Y_0} = -\frac{1}{\pi Y_0} \operatorname{Im} \int\limits_{X_1 + i0}^{X_0 + iY_0} \frac{df}{dZ} \frac{(Z - X_0)\, dZ}{\sqrt{(Z - Z_0)(Z - \overline{Z}_0)}}. \tag{6}$$

Here $X_1 + i0$ is a certain point on the symmetry axis X.

3. Mathematical Formulation of the Problem. We conformally map the regions corresponding to the IES in the planes Z and W onto a strip (Fig. 2). The machined surface ADB is mapped onto the real axis, and the cut $A'CB'$ onto the upper face of the strip. In this case, the solution of the problem of determining the function $W(Z)$ analytic in the IES can be represented in the parametric form $Z(\chi)$, $W(\chi)$. The boundaries of the IES are determined using the partial derivative $(\partial Z/\partial t)(\chi, t)$ by time discretization using a numerical method.

Thus, at each time t, three boundary-value problems are solved: to find three functions $W(\chi, t)$, $Z(\chi, t)$, and $(\partial Z/\partial t)(\chi, t)$, which are analytical inside the strip χ and satisfy certain boundary conditions.

The boundary condition for the function $W(\chi, t)$ is the above-mentioned equipotentiality condition for the anode (and, generally, cathode). On the boundary $A'CB'$ for a point cathode, $\Psi(X_0, 0) = I/\varkappa$.

The boundary condition for the function $Z(\chi, t)$ is the equality of the imaginary (or real) part of $Z(\chi, t)$ on the lower boundary of the strip $\chi = \sigma$ $(-\infty < \sigma < \infty)$ and the function $g_1(\sigma, t)$ known for each fixed value t. This boundary-value problem is solved analytically (using the Schwarz formula). At $t = 0$, the function $g_1(\sigma,0)$ is known from the initial condition, and the remaining values are obtained by time integration of the imaginary (or real) part of $(\partial Z/\partial t)(\sigma + i0, t)$. On the boundary $A'CB'$ for a point cathode, $\operatorname{Im} Z(\sigma + i/2, t) = 0$ and $\operatorname{Im} (\partial Z/\partial t)(\sigma + i/2, t) = 0$.

For the function $(\partial Z/\partial t)(\chi, t)$, the boundary conditions on the boundary ADB are given by the Faraday law (1). Let the tangent to the machined surface make angle θ with the x axis. Then, the projections of the displacement vectors of the point dZ and the strength E onto the normal to the surface can be calculated by the formulas $\Delta n = \operatorname{Im} (e^{-i\theta}\, dZ)$ and $E_n = \operatorname{Im} (e^{-i\theta}\, E)$. Since, on the boundary,

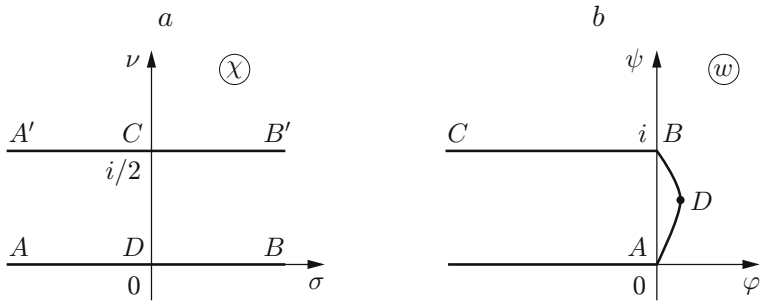

Fig. 2. Image of the IES in the planes of the parametric variable χ (a) and the complex potential w (b).

$$\frac{\partial Z}{\partial \sigma}(\sigma + i0, t) = \pm\Big|\frac{\partial Z}{\partial \sigma}\Big| \, \mathrm{e}^{i\theta},$$

the Faraday law (1) leads to the equality

$$\operatorname{Im}\Big(\overline{\frac{\partial Z}{\partial \sigma}}\,\frac{dZ}{dt}(\sigma + i0, t)\Big) = k \operatorname{Im}\Big(E\,\overline{\frac{\partial Z}{\partial \sigma}}\Big),$$

whence we have

$$\operatorname{Im}\Big(\overline{\frac{\partial Z}{\partial \sigma}}\,\frac{\partial Z}{\partial t} + \overline{\frac{\partial Z}{\partial \sigma}}\,\frac{\partial Z}{\partial \sigma}\,\frac{d\sigma}{dt}\Big) = k \operatorname{Im}\Big(\frac{\partial \Phi}{\partial X} + i\,\frac{\partial \Phi}{\partial Y}\Big)\overline{\frac{\partial Z}{\partial \sigma}}.$$

According to (2), condition (1) can be written in the final form as follows [17]:

$$\operatorname{Im}\Big(\overline{\frac{\partial Z}{\partial \sigma}}\,\frac{\partial Z}{\partial t}\Big) = -k\,\frac{1}{Y}\,\frac{\partial \Psi}{\partial \sigma}. \tag{7}$$

We introduce the dimensionless coordinates and time:

$$z = \frac{Z}{l}, \qquad x = \frac{X}{l}, \qquad y = \frac{Y}{l}, \qquad \tau = \lambda\,\frac{kI}{\varkappa l^3}\,t. \tag{8}$$

Here l is the characteristic size (independent of time), I is the value of the current in the electrochemical cell, and $\varkappa$ is the electrical conductivity of the electrolyte. The potential and stream function are represented as $\Phi = \varphi I/(\varkappa l)$ and $\Psi = \psi I/(\varkappa l^2)$, respectively. In the dimensional variables, equality (7) becomes

$$\frac{\partial x}{\partial \tau}\,\frac{\partial y}{\partial \sigma} - \frac{\partial y}{\partial \tau}\,\frac{\partial x}{\partial \sigma} = \frac{\lambda}{y}\,\frac{d\psi}{d\sigma}. \tag{9}$$

Equality (9) is the boundary condition for determining the analytic function $(\partial z/\partial \tau)(\chi, \tau)$ on the part of the boundary corresponding to the anode surface. As the characteristic size l it is convenient to choose the diameter of the groove D formed in the case of a large penetration of the tool electrode into the workpiece (according to the Faraday law $k/(\varkappa I) = V_0 \pi D^2/4$, where V_0 is the velocity of motion of the NE). The dimensionless time τ is chosen so that the dimensionless velocity of motion of the source is equal to $dx_C/d\tau = 1$. Then,

$$\lambda = \frac{\pi}{4}, \qquad l = D = \frac{2}{\sqrt{\pi}}\sqrt{\frac{kI}{\varkappa V_{et}}}, \qquad \tau = \frac{4}{\pi}\,\frac{kI}{\varkappa l^3}\,t.$$

4. Method of Solution of the Problem. In view of the aforesaid, the solution of the nonstationary axisymmetric problems includes three main stages: finding the conformal map of the region of the parametric variable onto the physical plane, determining the strength components by integral transformations of the analytic function, and calculating the partial time derivatives of the coordinates of the surface.

The problem of conformal mapping is solved as follows. As the range of the parametric variable $\chi = \sigma + i\nu$ it is convenient to use a strip of width $1/2$ with the correspondence of points indicated in Fig. 2.

The function mapping the plane χ onto the physical plane is sought in the form of the sum

$$z(\chi) = z_0(\chi) + z_\Delta(\chi).$$

As $\chi \to \infty$, the quantity $\operatorname{Re} z_\Delta(\chi) \to 0$. For $g > 0$, the function $z_0(\chi) = ig \sinh \pi\chi$ conformally maps the strip of the plane χ onto the left half-plane with a cut. In this case, the boundary $\chi = \sigma$ is mapped onto the surface ADB, and the boundary $\chi = \sigma + i/2$ onto the cut $A'CB'$. The point source is at the point $z_0(i/2) = -g$.

The function $z_\Delta(\chi)$ is determined as follows. The solution of the problem is sought at the nodal points σ_m $(m = 0, \ldots, n)$ on the boundary $\chi = \sigma$. The required quantities are the values $\operatorname{Re} z_\Delta(\sigma_m) = x_m$. We assume that, for $\sigma = \sigma_n$, $\operatorname{Re} z_\Delta(\sigma_n) = 0$ because, as $\sigma \to \infty$, the function $z_\Delta(\sigma)$ decreases exponentially. The values of $\operatorname{Re} z_\Delta(\sigma)$ at the points between the nodal points are found in the same way as is done in [18, 19], using a cubic spline $P(\sigma)$ which has two continuous derivatives.

To find the function $z_\Delta(\chi)$, we use the Schwarz formula [20] taking into account that $z_\Delta(\chi)$ is an analytic function which has [as well as $z_0(\chi)$] real values on the straight line $\operatorname{Im}\chi = 1/2$. Analytic continuation of the function $z_\Delta(\chi)$ onto a strip of unit width yields

$$z_\Delta(\chi) = -i2\sinh\pi\chi \int\limits_0^\infty P(\sigma)\,\frac{\cosh\pi\sigma}{\cosh^2\pi\sigma - \cosh^2\pi\chi}\,d\sigma. \tag{10}$$

The derivative $(dz_\Delta/d\chi)(\chi)$ is determined by differentiating (10):

$$\frac{dz_\Delta}{d\chi}(\chi) = -i2\cosh\pi\chi \int\limits_0^\infty \frac{dP}{d\sigma}(\sigma)\,\frac{\sinh\pi\sigma}{\cosh^2\pi\sigma - \cosh^2\pi\chi}\,d\sigma.$$

Specifying the condition $\operatorname{Re}[z_0(i/2) + z_\Delta(i/2)] = x_C$, we find the parameter g:

$$z(i/2) = -g + 2\int\limits_0^\infty P(\sigma)\,\frac{d\sigma}{\cosh\pi\sigma} = x_C.$$

The axisymmetric problem of determining the strength is solved by reducing it to an auxiliary plane problem, which is solved by conformally mapping the region corresponding to the IES in the plane of the complex potential (see Fig. 2b) onto the plane of the parametric variable χ (see Fig. 2a).

In the plane problem, the range of the complex potential is a half-strip of unit width:

$$w_0(\chi) = \frac{1}{\pi}\ln\Big(\tanh\frac{\pi}{2}\Big(\chi - \frac{i}{2}\Big)\Big). \tag{11}$$

The derivatives are given by the formulas

$$\frac{dw_0}{d\chi}(\chi) = \frac{i}{\cosh\pi\chi}, \qquad \frac{dw_0}{dz_0} = -\frac{1}{g\pi\cosh^2\pi\chi}, \qquad \frac{\partial^2 w_0}{\partial z_0\,\partial\chi}(\chi) = \frac{2\pi\sinh\pi\chi}{\cosh^3\pi\chi}. \tag{12}$$

In the auxiliary plane problem, the range of the complex potential is a curvilinear half-strip (see Fig. 2b) since, in this problem, the boundaries corresponding to the machined surface are nonequipotential. The variation in the potential on the boundary of the range of the solution of the plane problem is given by the boundary condition (3), where $f(z) = (dw/dz)(\chi)$ [16], $\Phi = \text{const}$, i.e., by the condition of equipotentiality of the boundary in the axisymmetric problem.

The dimensionless potential is sought in the form of the sum

$$\varphi(x,y) = \varphi_0(x,y) + \varphi_1(x,y) = -\frac{1}{4\pi}\,\frac{1}{\sqrt{(x+l)^2+y^2}} - \frac{1}{\pi}\operatorname{Im}\int\limits_0^{\sigma_0}\frac{\partial w}{\partial\sigma}(\sigma)\,\frac{d\sigma}{\sqrt{(z-z_0)(z-\overline{z}_0)}},$$

where $\varphi_0(x,y)$ is the potential of the point source located at a distance l on the left of the coordinate origin.

The strength components are calculated by formulas (5) and (6) with the replacement of the integration variable by σ and by changing the integration contour (since the integrand function is analytic in z):

$$\begin{aligned}
\frac{\partial}{\partial x}\,\varphi(x,y) &= -\frac{1}{4\pi}\frac{x+l}{[(x+l)^2+y^2]^{3/2}} - \frac{1}{\pi}\operatorname{Im}\int\limits_0^{\sigma_0}\frac{\partial^2 w}{\partial z\,\partial\sigma}(\sigma)\,\frac{d\sigma}{\sqrt{(z-z_0)(z-\overline{z}_0)}}\,,\\
\frac{\partial}{\partial y}\,\varphi(x,y) &= \frac{1}{4\pi}\,\frac{y^2}{[(x+l)^2+y^2]^{3/2}} + \frac{1}{\pi y}\operatorname{Im}\int\limits_0^{\sigma_0}\frac{\partial^2 w}{\partial z\,\partial\sigma}(\sigma)\,\frac{(z-x_0)\,d\sigma}{\sqrt{(z-z_0)(z-\overline{z}_0)}}\,.
\end{aligned} \tag{13}$$

The solution is sought in the form of the function

$$f_1(\chi) = \frac{\partial^2 w}{\partial z\, \partial \chi}(\chi).$$

This function should have properties similar to the properties of the function (12), i.e., for $\chi = \sigma + i0$, its real part should be an odd function of σ, and, for $\chi = \sigma + i/2$, the function $f_1(\sigma + i/2)$ should be real. Then, it can be continued analytically to the strip of unit width. In this case, $\operatorname{Re} f_1(\sigma + i) = \operatorname{Re} f_1(\sigma + i0)$.

The required parameters are the values of the real part of the function $\operatorname{Re} f_1(\sigma_m) = f_m$ at the nodal points σ_m $(m = 1, \ldots, n)$. For $\sigma = \sigma_0 = 0$, we have $\operatorname{Re} f_1(\sigma_0) = 0$ because the real part of f_1 is an odd function of σ, as well as the function $w_0(\chi)$ in (11). We assume that, for $\sigma = \sigma_n$, $\operatorname{Re} f_1(\sigma_n) = 0$ because, for $\sigma \to \infty$, function $f_1(\sigma)$ decreases exponentially. The values of $\operatorname{Re} f_1(\sigma)$ at the points located between the nodal points are found using a cubic spline.

To find the function $f_1(\chi)$, we use the Schwarz formula

$$f_1(\chi) = -i2 \cosh \pi\chi \int\limits_0^\infty S(\sigma)\, \frac{\sinh \pi\sigma\, d\sigma}{\cosh^2 \pi\sigma - \cosh^2 \pi\chi}.$$

In the solution using the collocation method, the condition of equipotentiality of the machined surface leads to the equations

$$F_m = \operatorname{Re}\Big[\Big(\frac{\partial\varphi}{\partial x} + i\,\frac{\partial\varphi}{\partial y}\Big)\,\overline{\frac{\partial z}{\partial\sigma}}(\sigma_m)\Big] = 0, \qquad m = 0, \ldots, n-1, \tag{14}$$

which is the equality of the tangential strength component to zero. Substituting the expression of $f_1(\sigma)$ written in terms of the spline and Schwarz formula into (13) and substituting the obtained expressions into (14), we have a system of linear (in the variables f_m) equations.

After the solution of the system of linear algebraic equations, the values of f_m are substituted into (13) to calculate $\partial\varphi/\partial x$ and $\partial\varphi/\partial y$.

The nonstationary problem is solved using discrete time steps Δ_τ. In each time step τ_j, we solve the problems of conformal mapping the strip of the parametric plane χ onto the physical plane z and determining the strength components $\partial\varphi/\partial x$, and $\partial\varphi/\partial y$. The conformal mapping problem is solved completely only for $\tau = 0$ because,after each time step, the values of the variables $x_m(\tau_j)$ are substituted into the spline and Schwarz integrals used.

After determining $\partial\varphi/\partial x$, $\partial\varphi/\partial y$, it is necessary to solve the third boundary-value problem: to find the partial derivative

$$\frac{\partial z_\Delta}{\partial\tau}(\chi, \tau_j) = \frac{\partial x_\Delta}{\partial\tau}(\chi, \tau_j) + i\,\frac{\partial y_\Delta}{\partial\tau}(\chi, \tau_j)$$

as an analytic function of the complex parameter χ. This problem has a unique solution, as well as the Riemann–Hilbert problem [17].

The derivative $(\partial z_\Delta/\partial\tau)(\chi, \tau_j)$ is calculated in the same way as the conformal map $z_\Delta(\chi, \tau_j)$. In each time step $\tau_j = j\Delta_\tau$, the required parameters are the values of $\operatorname{Re}(\partial z_\Delta/\partial\tau)(\sigma_m, \tau_j) = q_m$. The values of $\operatorname{Re}(\partial z_\Delta/\partial\tau)(\sigma, \tau_j)$ at the points located between the nodal points are found by using the cubic spline $R(\sigma, \tau)$.

To find the function $(\partial z_\Delta/\partial\tau)(\chi, \tau_j)$, we use a Schwarz formula similar to (10). For $\chi = i/2$, the same formula is used to determine $dg/d\tau$ from the specified values of $(dx_C/d\tau)(\tau) = 1$:

$$-\frac{dg}{d\tau}(\tau) + \frac{\partial x_\Delta}{\partial\tau}(i/2, \tau) = -\frac{dg}{d\tau} + 2\int\limits_0^\infty R(\sigma, \tau)\,\frac{d\sigma}{\cosh \pi\sigma} = \frac{dx_C}{d\tau} = 1.$$

The values of q_m are determined by the collocation method [18, 19] so that the boundary condition (9) is satisfied at the nodal points σ_m, $m = 1, \ldots, N$.

After solution of the system of linear algebraic equations and determination of the partial derivatives $\partial x_\Delta/\partial\tau = q_m$, a time step is made according to the predictor–corrector scheme of second-order accuracy.

Next, $\partial z_\Delta/\partial\sigma$, $\partial\varphi/\partial x$, $\partial\varphi/\partial y$, etc., are calculated.

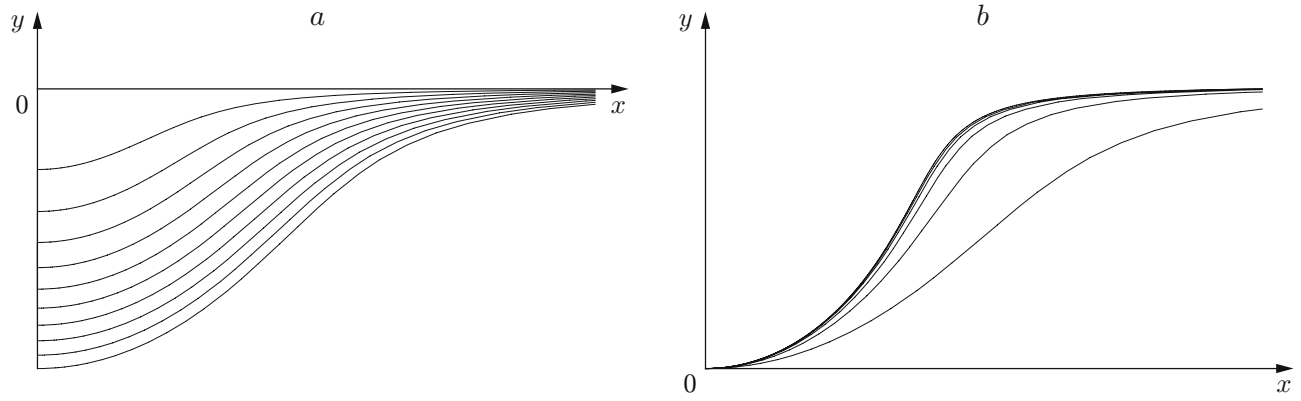

Fig. 3. Surface shape formed by machining with a stationary electrode: (a) initial stage of the process; (b) attainment of the stationary regime (the scale unit is the penetration depth).

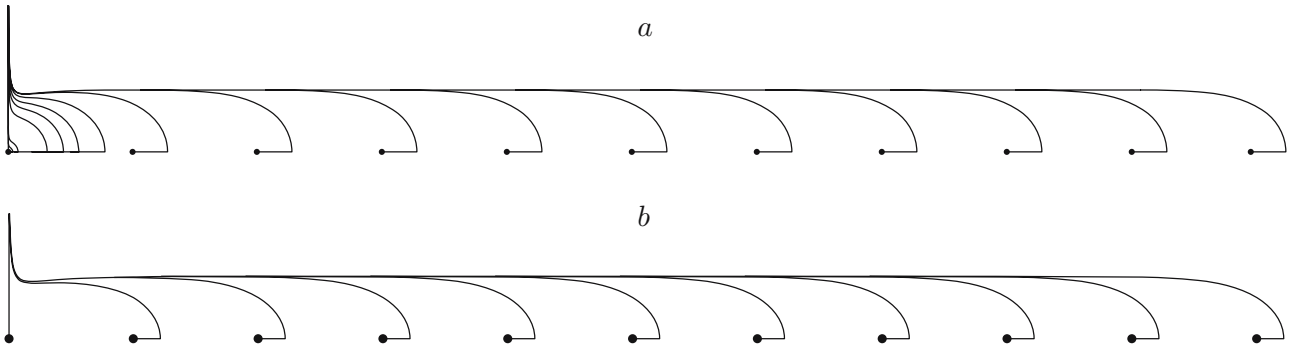

Fig. 4. Surface shape formed by machining with a moving electrode (at the beginning of the process, the gap between the electrode and the machined surface is equal to zero): (a) axisymmetric problem; (b) plane problem [19].

5. Results of Numerical Solution. We consider the machining process with a stationary PE located at distance l from the initially plane machined surface. In this case, the quantity l is a scale unity and the value of λ in (8), (9) is set equal to unity. Figure 3a shows the surface shape in the initial stage of the process (with a uniform time step), and Fig. 3b shows the attainment of a stationary regime (the step is proportional to the groove depth). It is evident that the shape of the groove is similar to that of the corresponding self-similar solution [21]. The scale of the figure is chosen such that the groove depth is always equal to unity.

Thus, during machining with a stationary NE, the machined surface of any shape takes a self-similar form, as in the plane case [18, 19]. Hence, the self-similar solution is an attractor.

The calculation results for the process of machining with a moving electrode for zero gap are given in Fig. 4. It is assumed that, initially, the process is self-similar. This assumption is based on the following facts: in the initial stage of the process, the dissolution rate is much higher than the velocity of motion of the NE; the self-similar shape is an attractor (according to the calculation results given in Fig. 3).

A stationary regime occurs near the NE. Thus, in the case of a moving NE, the attractor in its vicinity is the stationary solution. At the same time, near the beginning of the groove on the machined surface, a certain shape (further called the final shape) forms due to the removal of the PE from this region and the cessation of dissolution. A comparison shows that the solutions of the axisymmetric (see Fig. 4a) and plane (see Fig. 4b) problems are in good qualitative agreement.

6. Determining Parameters of Transitional Processes. Below, we study the formation of self-similar, stationary, and final shapes with increasing dimensionless time. Figure 5a gives a curve of the product of the curvature K and depths l of the groove on the machined surface (see Fig. 3) versus the logarithm of the dimensionless time τ for a stationary NE. Figure 5b (curve 1) gives a curve of the decimal logarithm of the relative

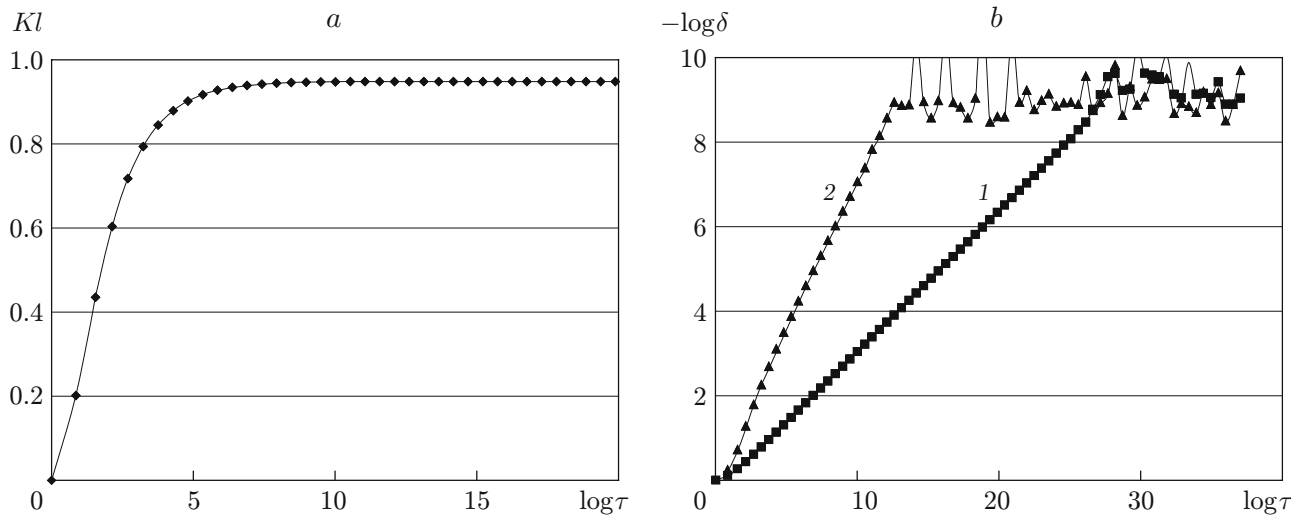

Fig. 5. Dependences of Kl (a) and $-\log\delta$ (b) on $\log\tau$ during the formation of a self-similar surface shape: 1) main component of the dependence; 2) second component of the dependence.

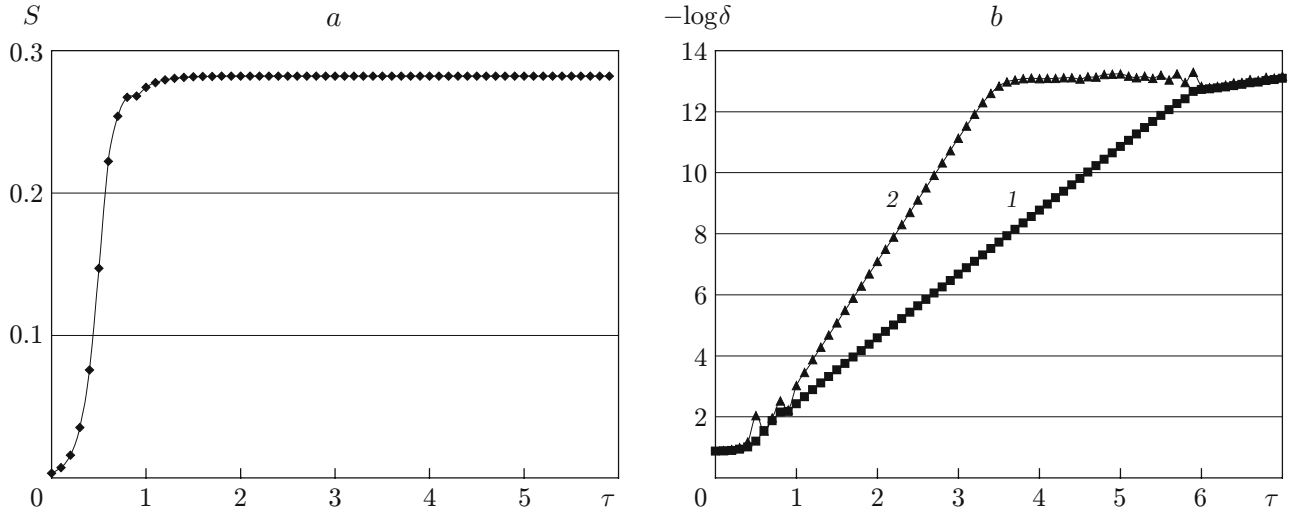

Fig. 6. Time dependences of the gap size (a) and the quantity $-\log\delta$ (b) during formation of a stationary gap: 1) main component of the dependence; 2) second component of the dependence.

difference $-\log\delta = -\log|K(\tau)l(\tau)/Kl^* - 1|$ from $\log\tau$ ($Kl^* = 0.948\,474\,795 \pm 10^{-8}$ is the limiting (as $\tau\to\infty$) value obtained independently of the solution of the self-similar problem [21]). It is evident that this dependence is nearly linear. As a result of filtration [22] of the data of the nonstationary problem, the obtained values correspond to the limiting value to within 8–9 places.

The angular coefficient of the linear dependence was estimated using the filtration method [22]. The calculations gave the angular coefficient of the logarithmic dependence $k_\tau = 1/3$ (relative calculation error $\delta_k = 10^{-5}$). The suppression of the main component of the dependence by filtration revealed the presence of the component with a doubled value of the angular coefficient (curve 2 in Fig. 5b).

Thus, from the numerical experiment, it follows that the time dependence of the quantity Kl^* is approximated by the function

$$K(\tau)l(\tau) = Kl^*(1 - c\tau^{-1/3}).$$

We note that the self-similar solution is characterized by the power-law dependence $l(\tau) = l_0\tau^{1/3}$.

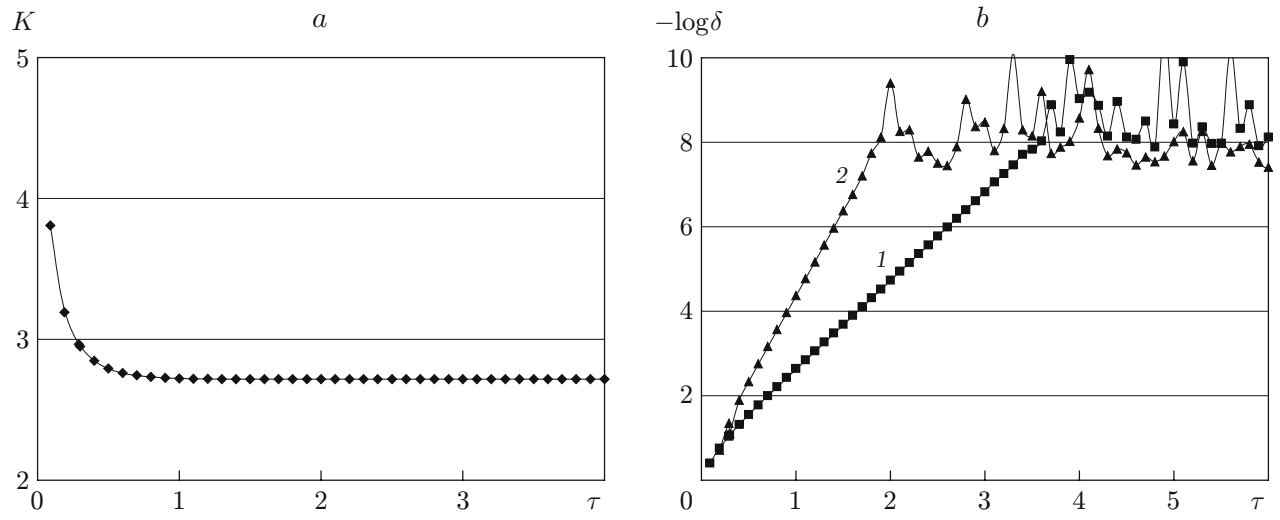

Fig. 7. Time dependences of the curvature (a) and the quantity $-\log\delta$ (b) during formation of a stationary surface shape: 1) main component of the dependence; 2) second component of the dependence.

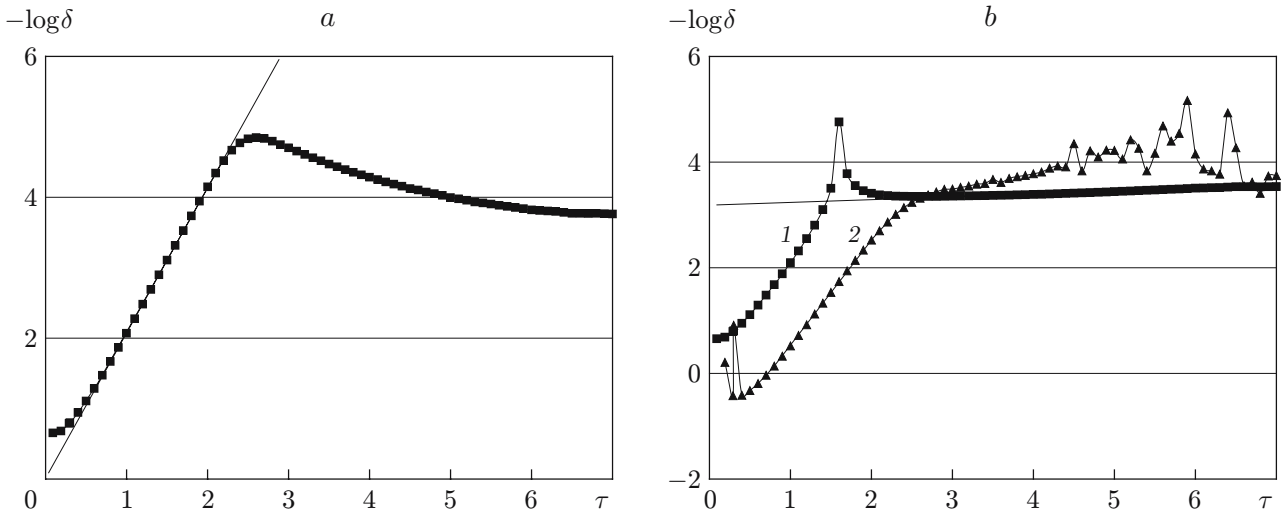

Fig. 8. Time dependence of the quantity $-\log\delta = -\log|K(\tau)/K^* - 1|$ (a) and the slow component of this dependence (b) during formation of the maximum value of the curvature of the final surface shape: 1) main component of the dependence; 2) second component of the dependence.

Figure 6a shows the dependence of the gap size between a moving PE (see Fig. 4a) and the nearest point of the machined surface on the dimensionless time τ. Figure 6b gives the dependence of the quantity $-\log\delta = -\log|S(\tau)/S^* - 1|$ on the dimensionless time τ (S is the gap size and $S^* = 0.282186858398 \pm 10^{-12}$ is the stationary gap size obtained by solving the stationary problem [21]). It is evident that this dependence is nearly linear, i.e., the law of formation is nearly exponential:

$$S(\tau) = S^*(1 - c \cdot 10^{-k_\tau \tau}).$$

From the calculations, it follows that the angular coefficient of the logarithmic dependence is $k_\tau = 2.088805 \pm 10^{-6}$. The angular coefficient for the second component (curve 2 in Fig. 6b) is approximately twice this value.

Figure 7a gives a curve of the curvature of the machined surface at the point the nearest to the PE versus the dimensionless time τ, and Fig. 7b gives a curve of $-\log\delta = -\log|K(\tau)/K^* - 1|$ versus τ (K is the curvature and $K^* = 2.716\,660 \pm 10^{-6}$ is the stationary curvature). From the calculations, it follows that the angular coefficient is $k_\tau = 2.0888 \pm 2 \cdot 10^{-4}$.

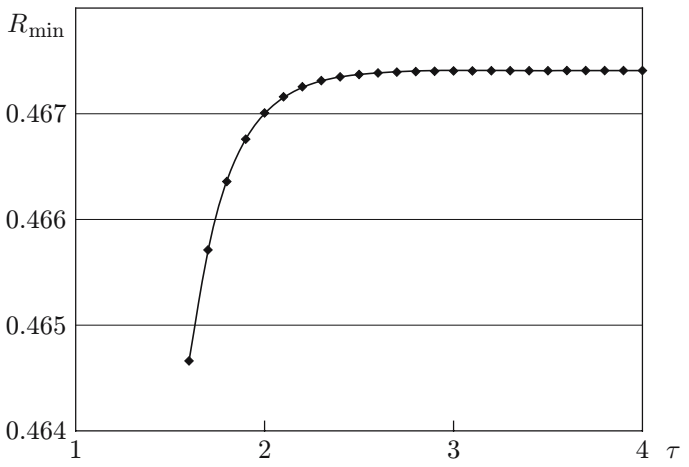

Fig. 9. Minimum hole radius versus time.

Figure 8 gives a curve of $-\log\delta = -\log|K(\tau)/K^* - 1|$ versus τ for $K^* = -15.065 \pm 5 \cdot 10^{-3}$ during formation of the final surface shape. From the calculation results, the angular coefficient is $k_\tau = 2.08 \pm 2 \cdot 10^{-2}$. Increasing the calculation accuracy revealed a new effect not noticeable earlier due to error: the curvature modulus first increases to a value of $-K \approx 15.073$ and then decreases to a value of $-K \approx 15.065$ (Fig. 8a). The characteristic rate of decrease in the values of $-K$ is much lower than the characteristic rate of their increase. In this case, the angular coefficient is $k_\tau \approx 0.07$ (in Fig. 8a, $k_\tau \approx 2.08$). After the suppression of this component of the dependence $-\log\delta(\tau)$, it is evident that there is a second component (curve 2 in Fig. 8b).

For zero initial gap, narrowing of the hole in the final zone of the machined surface (see Fig. 4a) was observed. The dependence of the minimum hole radius in the machined material versus time is given in Fig. 9. The angular coefficient was found to be $k_\tau = 2.089 \pm 2 \cdot 10^{-3}$.

Conclusions. A method for the numerical solution of nonstationary axisymmetric Hele-Shaw problems using integral transformations of analytic function was proposed. The results of numerical calculations confirmed the high efficiency of the method.

The studies of the time characteristics of shape formation in the stationary and final zones showed that the time constant k_τ had identical values within accuracy for all dependences considered. The calculation accuracy of the final shape was lower than that of the stationary shape, and the spread in the values of k_τ is therefore larger. Nevertheless, it can be argued that, in transition to the stationary and final surface shapes, no difference between the values of k_τ was found. Invariance of this quantity for various conditions of establishment of the stationary process is unquestionable. However, the fact that this quantity determines the rate of formation of the final shape is difficult to predict in advance.

REFERENCES

1. P. Ya. Polubarinova-Kochina, "Nonstationary motion in filtration theory," *Prikl. Mat. Mekh.*, **9**, 79–90 (1945).
2. P. Ya. Polubarinova-Kochina, *Theory of Groundwater Movement*, Princeton Univ. Press, Princeton (1962).
3. L. A. Galin, "Nonstationary free-boundary filtration," *Dokl. Akad. Nauk SSSR*, **47**, 246–249 (1945).
4. J. A. McGeough, *Principles of Electrochemical Machining*, Chapman and Hall, London (1974).
5. J. A. McGeough and H. Rasmussen, "On the derivation of the quasi-steady model in electrochemical machining," *J. Inst. Math. Appl.*, **13**, 13–21 (1974).
6. S. D. Howison, "Complex variable methods in Hele-Shaw moving boundary problems," *Eur. J. Appl. Math.*, **3**, 209–224 (1992).
7. S. D. Howison and J. R. King, "Explicit solutions to six free boundary problems in fluid flow and diffusion," *IMA J. Appl. Math.*, **42**, 155–175 (1989).

8. S. D. Howison, J. R. Ockendon, and A. A. Lacey, "Singularity development in moving boundary problems," *Quart. J. Mech. Appl. Math.*, **38**, 343–360 (1985).
9. P. Novak, I. Rousaz, A. Kimla, et al., "Mathematical simulation of electrochemical machining," in: *Proc. of the Int. School ECMM-88*, Lubnevitsy Univ., Lubnevitsy (1988), pp. 100–115.
10. J. Pandey, "Finite element approach to the two dimensional analysis of ECM," *J. Precision Eng.*, **1**, 23–28 (1980).
11. S. Christiansen and H. Rasmussen, "Numerical solutions for two-dimensional annular electrochemical machining problems," *J. Inst. Math. Appl.*, **18**, 295–307 (1976).
12. A. West, C. Madore, M. Moltosz, and D. Landolt, "Shape changes during through-mask electrochemical micromachining of thin metal films," *J. Electrochem. Soc.*, **2**, No. 139, 499–506 (1992).
13. V. M. Volgin and A. D. Davydov, "Modeling of multistage electrochemical shaping," *J. Mater. Proc. Technol.*, **149**, 466–471 (2004).
14. M. Purcar, L. Bortels, B. Van den Bossche, and J. Deconinck, "3D electrochemical machining computer simulations," *J. Mater. Proc. Technol.*, **149**, 472–478 (2004).
15. G. N. Polozhii, *Generalization of the Theory of Analytic Functions of a Complex Variable* [in Russian], Kiev. Gos. Univ., Kiev (1965).
16. V. P. Zhitnikov, *Solution of Plane and Axisymmetric Problems Using Methods of the Theory of Functions of a Complex Variable* [in Russian], Ufa State Avia. Tech. Univ., Ufa (1994).
17. V. P. Zhitnikov, O. R. Zinnatullina, and G. I. Fedorova, "Analytical solution of the Riemann–Hilbert problem with the conditions occurring in plane and axisymmetric Hele-Shaw problems," *Vest. Ufim. Gos. Aviats. Univ.*, **7**, No. 2, 149–154 (2006).
18. V. P. Zhitnikov, O. R. Zinnatullina, and G. I. Fedorova, and A. V. Kamashev, "Simulation of nonstationary processes of electrochemical machining," *J. Mater. Proc. Technol.*, **149**, 398–403 (2004).
19. V. P. Zhitnikov, G. I. Fedorova, N. M. Sherykhalina, and A. R. Urakov, "Numerical investigation of nonstationary electrochemical shaping based on an analytical solution of the Hele-Shaw problem," *J. Eng. Math.*, **55**, No. 1–4, 255–276 (2006).
20. M. A. Lavrent'ev and B. V. Shabat, *Methods of the Theory of Functions of a Complex Variable* [in Russian], Nauka, Moscow (1973).
21. V. P. Zhitnikov, O. R. Zinnatullina, and G. I. Fedorova, "Self-similar Hele-Shaw problems," in: *Proc. of Workshop on Computer Sciences and Information Technologies* (CSIT2007), Vol. 2, Ufa State Avia. Tech. Univ., Ufa (2007), pp. 192–198.
22. N. M. Sherykhalina, "Methods of processing the results of numerical experiments for increasing their accuracy and reliability," *Vestnik Ufim. Gos. Aviats. Univ.*, **9**, No. 2, 127–137 (2007).